# Coupled-Reaction-Channels Study of $(h, t)$ Reactions*

W. R. Coker, T. Udagawa, and H. H. Wolter†
*Center for Nuclear Studies, University of Texas, Austin, Texas 78712*
(Received 19 October 1972)

We have developed a formulation of the theory of multichannel nuclear reactions which permits practical and realistic numerical calculations in which a number of different reaction channels are coupled, assuming a zero-range approximation for the effective coupling and neglecting effects arising from the non-orthogonality of different reaction channels. A computer program, JUPITER-4, has been written embodying this coupled-reaction-channel formulation, and as a specific application we present analyses of the $(h,\alpha)$-$(\alpha,t)$ or pickup-stripping contributions to $(h,t)$ reactions, for the specific cases of $^{48}$Ca$(h,t)^{48}$Sc and $^{40}$Ar-$(h,t)^{40}$K. We pay particular attention to the interplay and interference of direct and pickup-stripping amplitudes, and try to identify general tendencies. Finally, we give simple sum rules which aid in predicting the nature of the interference for specific spins of intermediate and final nuclear states.

## I. INTRODUCTION

The reactions $(h, t)$ and $(p, n)$ at reasonable energies have customarily been interpreted as occurring through a direct, one-step charge-exchange process.[1-4] Evidence for this mechanism is the strong population of isobaric analog resonances by such reactions. However, much recent experimental evidence suggests that a simple direct-reaction process is not necessarily the dominant reaction mechanism, particularly for $(h, t)$ and that the usual distorted-wave Born approximation (DWBA) is inadequate.[5-11] (The symbol $h$ stands for the helion, the nucleus of the mass-3 helium atom.)

For example, the angular distributions for $(h, t)$ population of the $J^\pi = 0^+$ antianalog state in a variety of nuclei do not have an $l = 0$ pattern, but can be fitted in shape by an $l = 1$ DWBA calculation.[6] A persistent shift, to backward angles, of the experimental angular distributions relative to DWBA calculations has been observed generally for residual $T_<$ states of any $J$.[6-8] A serious anomaly in magnitude is observed, such that $(h, t)$ cross sections for $4^+$ and $6^+$ $T_<$ states have magnitudes 1 or 2 orders greater than expected on the basis of DWBA calculations, using microscopic form factors.[5] These discrepancies are not removed by more sophisticated DWBA approaches including a tensor force, exchange terms, etc.[9] Further, a strong energy dependence is noted in the microscopic or macroscopic form factor when angular distributions are fitted at several energies.[10] Finally, it is noted that arbitrarily introducing a complex part to the microscopic form factor often improves the calculated DWBA angular distribution in shape, relative to the data.[11]

All such observations point to a multistep mechanism for $(h, t)$.[12-14] Toyama,[13] and the present authors[14] have investigated the effect of the pickup-stripping mechanism for $(h, t)$, namely, $(h, \alpha)$, $(\alpha, t)$ processes. Toyama calculated cross sections for $^{48}$Ca$(h, t)^{48}$Sc leading to the $(f_{7/2}^{-1}f_{7/2})$, $0^+$ to $6^+$ states in $^{48}$Sc, assuming a pure $(h, \alpha)$, $(\alpha, t)$ mechanism. He was able to account for the relative magnitudes of all four states, as well as to obtain excellent shape fits to the available data at two incident energies. He also found a negligible contribution from $(h, d)$, $(d, t)$. We have previously shown that to explain the angular shift in the $^{40}$Ar-$(h, t)^{40}$K $0^+$-antianalog-state angular distribution, and the relative magnitudes of $0^+$-analog-state and $0^+$-antianalog-state cross sections, one has to assume both direct *and* pickup-stripping mechanisms, with careful treatment of the interference between them.[14]

The $(h, t)$ cross sections are generally 1 or 2 orders of magnitude smaller than typical inelastic scattering cross sections for population of collective states, and typical single-nucleon-transfer-reaction cross sections. It is then not surprising if two-step processes can play an important role in $(h, t)$. Important contributions from inelastic processes in entrance and exit channels have previously been found for $(p, t)$ reactions, which have cross sections comparable in magnitude to $(h, t)$ reactions.[15] The possibility of successive single-nucleon-transfer mechanisms for two-nucleon-transfer reactions has not to date been studied, though $(p, h)$ and $(d, \alpha)$ reactions could have important contributions from such mechanisms.

It is of great interest to investigate in a systematic way the contributions of successive specific nuclear reactions to a given reaction. We have developed a program JUPITER 4 which solves a set of coupled radial Schrödinger equations for

different reaction channels and system mass partitions.[16-18] The purpose of the present work is to present the multichannel formulation on which the program is based, and to present a specific application to the analysis of $^{40}$Ar$(h, t)^{40}$K and $^{48}$Ca$(h, t)^{48}$Sc reaction data.

In Sec. II we give the coupled-reaction-channels (CRC) formalism, which is reduced to easily calculable form[19] by neglecting non-orthogonality of different channels and making a zero-range approximation for the effective channel-coupling potentials, as in DWBA.[1] In Sec. III we summarize the effective channel-coupling potentials, or form factors, needed for one-particle transfer, inelastic scattering, and charge exchange. Careful attention is paid to relative phases, without detailed knowledge of which a correct treatment of competing mechanisms is impossible.

In Sec. IV, we study the $^{48}$Ca$(h, t)^{48}$Sc reaction,[20] extending work of Toyama to include both direct and two-step mechanisms. Since the antianalog $0^+$ state is not observed in the $^{48}$Ca data, we also have analyzed $^{40}$Ar$(h, t)^{40}$K data.[6] Finally, general and specific conclusions which can be drawn from the analyses are summarized in Sec. V.

## II. FORMULATION

### A. Coupled-Reaction-Channels Formalism

The sort of reaction process considered in this paper may be symbolized by $a+A \to b+B \to c+C\ldots$ where each step of the process, for instance $a+A \to b+B$, can be any nuclear reaction, such as one- or many-nucleon transfer, inelastic scattering, etc. To follow the process from initial state, through intermediate states, to a given final state we introduce the label $\alpha \equiv \{l_a j_a s_a; aA\}$ denoting the set of the usual channel quantum numbers $l_a j_a s_a$, as well as the particular mass partition, $a+A$, involved. No confusion will arise if a label such as $A$ is also used to specify the set of internal quantum numbers of nucleus $A$.

The total state function for the system may be written as

$$\Psi^{(+)} = \sum_{J\alpha} r_\alpha^{-1} \chi_\alpha^J(r_\alpha) \Phi_\alpha^{JM}, \tag{1}$$

where $\chi_\alpha^J(r_\alpha)$ is the partial distorted-wave function and $\Phi_\alpha^{JM}$ is the channel state function conventionally defined as

$$\Phi_\alpha^{JM} = [\mathcal{Y}_{l_a s_a j_a} \phi_a \otimes \phi_{J_A}]_{JM}. \tag{2}$$

Here $\mathcal{Y}_{l_a s_a j_a}$ is the spin-angle function,

$$\mathcal{Y}_{l_a s_a j_a m_{ja}} = \sum \langle l_a m_{la}\, s_a m_a | j_a m_{ja}\rangle i^{l_a} Y_{l_a m_{la}} \chi_{s_a m_a}. \tag{3}$$

As usual, $Y_{l_a m_{la}}$ is a spherical harmonic and $\chi_{s_a m_a}$ is the spin state function of the projectile $a$. Also, $\phi_a$ and $\phi_A$ (or $\phi_{J_A}$) in Eq. (2) are, respectively, the spatial and isospin parts of the internal state function of the projectile $a$ and the internal state function of the nucleus $A$.

If one now introduces the product of the internal state functions $\chi_{s_a m_a}$, $\phi_a$, and $\phi_A$, namely

$$\psi_\alpha \equiv \chi_{s_a m_a} \phi_a \phi_A. \tag{4a}$$

Then $\psi_\alpha$ satisfies

$$H_\alpha \psi_\alpha = \epsilon_\alpha \psi_\alpha, \tag{4b}$$

where $H_\alpha$ may be called the intrinsic Hamiltonian of the channel $\alpha$.

The equation for the radial distorted-wave function, $\chi_\alpha^J(r_\alpha)$, is derived from the Schrödinger equation for the total wave function $\Psi^{(+)}$;

$$H\Psi^{(+)} = E\Psi^{(+)}, \tag{5}$$

where $H$ is the total Hamiltonian of the system, which may be rewritten

$$\begin{aligned} H &= H_\alpha + T_\alpha + V_\alpha \\ &= H_\alpha + T_\alpha + U_\alpha + (V_\alpha - U_\alpha). \end{aligned} \tag{6}$$

Here, $T_\alpha$ is the kinetic energy of the relative motion between $a$ and $A$, and $V_\alpha$ is the interaction potential between them. In the second line in Eq. (6), the distorting one-body optical potential, $U_\alpha$ has also been introduced. Inserting Eqs. (6) and (1) into (5), we get

$$\begin{aligned} (H_\alpha + T_\alpha + U_\alpha - E) \sum_{J\beta} r_\beta^{-1} \chi_\beta^J(r_\beta) \Phi_\beta^{JM} \\ = -(V_\alpha - U_\alpha) \sum_{J\beta} r_\beta^{-1} \chi_\beta^J(r_\beta) \Phi_\beta^{JM}. \end{aligned} \tag{7}$$

The equation for $\chi_\alpha^J$ is then obtained by projecting out a given component $\Phi_\alpha^J$ by multiplying it on the left-hand side of the above equation and performing an integration over all the internal variables in the channel $\alpha$. A complication can arise if effects due to the non-orthogonality of the channel wave functions $\Phi_\alpha^J$ are important – one will not then be able to project out a single term in the sum over $J, \beta$. In the present work, however, we neglect the non-orthogonality of the basis states and simply set

$$\begin{aligned} \langle \Phi_\alpha^J | H_\alpha + T_\alpha + U_\alpha - E | \Psi^{(+)} \rangle \\ \approx (T_\alpha + U_\alpha - E_\alpha) r_\alpha^{-1} \chi_\alpha^J(r_\alpha), \end{aligned} \tag{8}$$

with $E_\alpha = E - \epsilon_\alpha$. Using this approximation, one

gets

$$(T_\alpha + U_\alpha - E_\alpha) r_\alpha^{-1} \chi_\alpha^J(r_\alpha) = -\sum_{J\beta} \langle \Phi_\alpha^J | V_\alpha - U_\alpha | \Phi_\beta^J \rangle r_\beta^{-1} \chi_\beta^J(r_\beta) . \tag{9}$$

This is the CRC equation for the distorted waves, $\chi_\alpha^J$, and has exactly the same form as obtained for the coupled-channel equations for inelastic scattering.[19]

A more rigorous derivation of the coupled-channel equation, taking into account non-orthogonality, has been given by Omura *et al.*,[16] and also by Takeuchi-Goldfarb.[17] A numerical estimate of the effects of non-orthogonality in pertinent cases has also been given in Ref. 17, where it is indicated that the effects are rather small.

To put Eq. (9) into a more convenient form for numerical calculations, we introduce the usual zero-range approximation,[1] with $\overline{V}_\beta = V_\beta - U_\beta$, in the spirit of direct-reaction theory. In the zero-range approximation, one can write[1]

$$J\langle \phi_b \chi_{s_b m_b} \phi_{J_B M_B} | \overline{V}_\alpha | \phi_a \chi_{s_a m_a} \phi_{J_A M_A} \rangle = \sum_{lsj} i^{-l} A_{lsj}^{BA} F_{lsj}^{BA}(r_\alpha) Y_{lm_l}^*(\hat{r}_\alpha) \delta\left(\vec{r}_\beta - \frac{A}{B}\vec{r}_\alpha\right) \langle J_A M_A jm_j | J_B M_B \rangle (-)^{s_b - m_b} \langle s_a m_a s_b - m_b | sm_s \rangle \langle lm_l sm_s | jm_j \rangle , \tag{10}$$

where $J$ is the Jacobian of the transformation of the final channel coordinates to those in the initial channel, and $l$, $s$, and $j$ are the transferred orbital, spin, and total angular momenta, respectively. Further $A_{lsj}^{BS}$ and $F_{lsj}^{BA}$ are, respectively, the spectroscopic amplitude and the form factor. Inserting (10) into (9), after a little algebra, one can show that

$$D_\beta(\rho_\beta)\chi_\beta^J(\rho_\beta) = \sum_\gamma \mathfrak{V}_{\beta\gamma}^J(\rho_\gamma)\chi_\gamma^J(\rho_\gamma) , \tag{11}$$

where

$$D_\beta(r) \equiv \frac{\hbar^2}{2\mu_\beta}\left(\frac{d^2}{dr^2} - \frac{l_b(l_b+1)}{r^2}\right) - U_\beta(r) + E_\beta . \tag{12}$$

The coordinate $\rho_\beta$ is a convenient choice because of the zero-range assumption. It is given by $\rho_\beta \equiv (A/B)r$, $\rho_\gamma \equiv (A/C)r$, etc. Note that here $A$ is used to denote specifically the mass of the target nucleus in the incident channel. Also,

$$\mathfrak{V}_{\beta,\gamma}^J(r) = \sum_{lsj} (B/C)^2 \tilde{A}_{lsj}^{BC} A(l_b s_b j_b J_B, l_c s_c j_c J_C; lsjJ) F_{lsj}^{BC}(r) , \tag{13}$$

where

$$\tilde{A}_{lsj}^{BC} \equiv \hat{J}_B A_{lsj}^{BC} , \quad \hat{J} \equiv (2J+1)^{1/2} \tag{14}$$

and

$$A(l_b s_b j_b J_B, l_c s_c j_c J_C; lsjJ) \equiv (4\pi)^{-1/2}(-)^{j_c + J_C - J} i^{l_c + l_b - l} \times \hat{l}_c \hat{l}_b \hat{j}_c \hat{j}_b \hat{s} \hat{j} \langle l_c 0 l_b 0 | l0 \rangle W(j_c j_b J_C J_B; jJ) \begin{pmatrix} l_c & s_c & j_c \\ l_b & s_b & j_b \\ l & s & j \end{pmatrix} . \tag{15}$$

A more explicit form for the spectroscopic amplitude, $\tilde{A}_{lsj}^{BC}$, and the form factor, $F_{ljs}^{BC}$ will be given in the next section for the one-nucleon-transfer, inelastic, and charge-exchange reactions.

### B. Transition Amplitude and Cross Section

The transition amplitude for the reaction can be given in terms of the $C$ matrix $C_{\beta,\alpha}^J$,[19] which is determined from the asymptotic form of the partial wave $\chi_\beta^J$:

$$\chi_{\beta,\alpha}^J \equiv \chi_\beta^J \to \hat{l}_a e^{i\sigma_{l_a}} F_{l_a} \delta_{l_a l_b} \delta_{j_a j_b} \delta_{A,B} + \hat{l}_b [k_a/k_b][v_a/v_b]^{1/2} e^{i\sigma_{l_b}} C_{\beta,\alpha}^J (G_{l_b} + iF_{l_b}) , \tag{16}$$

where $\chi^J_\beta$ is denoted by $\chi^J_{\beta,\alpha}$ in order to express explicitly the boundary condition of an incoming wave in the channel $\alpha$. $F_l$ and $G_l$ are the regular and irregular Coulomb functions, $k$ is the channel wave number, and $\sigma_l$ is the Coulomb phase shift.

With the $C$ matrix, the transition amplitude can be given as[19]

$$T_{bBm_bM_B,aAm_aM_A}=\sum_l C^{l(m_l)}_{bBm_bM_B,aAm_aM_A}P_{l|m_l|}(\cos\theta)\,, \tag{17}$$

where

$$C^{l(m_l)}_{bBm_bM_B,aAm_aM_A}=\sum_{Jj_b}(1/k_b)(2l+1)e^{2i\sigma_l}(-)^{(m_l+|m_l|)/2}[(l-|m_l|)!/(l+|m_l|)!]^{1/2}$$
$$\times\langle j_bm_{j_b}J_BM_B|JM\rangle\langle lm_ls_bm_b|j_bm_{j_b}\rangle\sum_{l_aj_a}\langle l_a0s_am_a|j_am_a\rangle\langle j_am_aJ_AM_A|JM\rangle C^J_{\beta,\alpha}\,. \tag{18}$$

The cross section is then written as

$$\frac{d\sigma}{d\Omega}=[(2J_A+1)(2s_a+1)]^{-1}\sum_{m_aM_Am_bM_B}|T_{bBm_bM_B,aAm_aM_A}|^2\,. \tag{19}$$

### C. First- and Second-Order Solutions

The lowest-order approximate solution of the CRC equations is obtained if they are solved by iteration and the iteration is stopped after the first. For a one-step direct reaction $a+A\to b+B$, this first-order solution gives a transition amplitude equivalent to that of the usual DWBA. For a two-step process, $a+A\to c+C\to b+B$, the first-order solution gives a transition amplitude corresponding to the second DWBA (second-order DWBA), and so on.

An alternate way to generate such a first-order solution is to solve the coupled equations exactly, but to include only couplings such as $\mathcal{U}^J_{\gamma\alpha}$ and $\mathcal{U}^J_{\beta\gamma}$, ignoring the "backward" transitions induced by $\mathcal{U}^J_{\alpha\gamma}$ and $\mathcal{U}^J_{\gamma\beta}$ [see Eq. (11)].

Both methods of obtaining the first-order solution have been used in our calculations. We have also, of course, solved the coupled equations exactly to all orders for certain cases. We have constructed a CRC program using a compact version of Tamura's JUPITER-1[21] as a starting point. Our CRC program, JUPITER-4, contains, however, the additional iterative method as an option, unlike JUPITER-1.

In the sections to follow we apply the CRC formalism to the $(h, t)$ reaction. The intermediate channels considered in the $(h, t)$ are those reached by $(h, \alpha)$ and depopulated by $(\alpha, t)$ processes. As we will demonstrate in Sec. 5, the second DWBA is found to give results in good agreement with exact CRC calculations, and many of the calculations reported here were made in second DWBA to save computation time.

## III. FORM FACTORS AND SPECTROSCOPIC AMPLITUDES

It will already have been noticed from Eq. (10) that the zero-range channel-coupling potential is identical to the effective transition potential of the familiar DWBA amplitude, so that the form factor and spectroscopic amplitude have their usual meaning. Methods of computing such form factors and spectroscopic amplitudes have been discussed by many authors, for one-nucleon or many-nucleon stripping and pickup reactions, inelastic scattering, and charge-exchange reactions.[1-3] The only new feature is that now, in CRC, one must pay careful attention to phases and signs of these quantities, which have commonly been ignored. In CRC, interference effects are tremendously important.

For purposes of the numerical calculations presented here and elsewhere, we have paid particular attention to the spin-isospin-state-function overlap integrals which occur in Eq. (10) and we show an explicit calculation here. To have a fixed phase convention, we have consistently used for all reactions the following spin-isospin state functions:

$$|N\rangle=c^\dagger_{m\nu}|0\rangle\,,\quad \nu=\begin{cases}\frac{1}{2}\text{ for }n\\ -\frac{1}{2}\text{ for }p\end{cases}, \tag{20a}$$

$$|d\rangle=\mathcal{A}^\dagger_{1m00}|0\rangle\,, \tag{20b}$$

$$|T\rangle=b^\dagger_{m\nu}|\alpha\rangle\,,\quad \nu=\begin{cases}\frac{1}{2}\text{ for }t\\ -\frac{1}{2}\text{ for }h\end{cases}, \tag{20c}$$

$$|\alpha\rangle=\frac{1}{\sqrt{3}}[\mathcal{A}^\dagger_{10}\mathcal{A}^\dagger_{10}]_{0000}|0\rangle\,, \tag{20d}$$

TABLE I. $D_0(ab)$ factor for various one-particle-transfer processes. In columns 2 and 3, the values of $D_0$ and the spectroscopic overlap integral are also shown.

| $(a,b)$ | $D_0$ ($10^2$ MeV fm$^{3/2}$) | $\hat{s}^{-1}\langle s_a \| \{c^\dagger\} \| s_b\rangle$ | $D_0(ab)$ ($10^2$ MeV fm$^{3/2}$) |
|---|---|---|---|
| $(d,p)$ | −1.257 | $(\frac{3}{2})^{1/2}$ | −1.540 |
| $(p,d)$ | | $(\frac{3}{2})^{1/2}$ | −1.540 |
| $(d,n)$ | −1.257 | $-(\frac{3}{2})^{1/2}$ | +1.540 |
| $(n,d)$ | | $(\frac{3}{2})^{1/2}$ | −1.540 |
| $(t,d)$ | −1.836 | $-(\frac{3}{2})^{1/2}$ | +2.249 |
| $(d,t)$ | | $(\frac{3}{2})^{1/2}$ | −2.249 |
| $(h,d)$ | −1.728 | $-(\frac{3}{2})^{1/2}$ | +2.117 |
| $(d,h)$ | | $-(\frac{3}{2})^{1/2}$ | +2.117 |
| $(\alpha,h)$ | −4.796 | −1 | +4.769 |
| $(h,\alpha)$ | | 1 | −4.769 |
| $(\alpha,t)$ | −4.796 | 1 | −4.769 |
| $(t,\alpha)$ | | 1 | −4.769 |

where

$$\mathcal{A}^\dagger_{sm\tau\nu} = \frac{1}{\sqrt{2}} \sum \langle \tfrac{1}{2} m_1 \tfrac{1}{2} m_2 \,|\, sm\rangle \langle \tfrac{1}{2}\nu_1 \tfrac{1}{2}\nu_2 \,|\, \tau\nu\rangle c^\dagger_{m_1\nu_1} c^\dagger_{m_2\nu_2}, \tag{21}$$

$$b^\dagger_{m\nu} = (-)^{1/2+m+1/2+\nu} c_{-m-\nu}. \tag{22}$$

Here, $c^\dagger_{m\nu}$ is the creation operator of a particle with spin and isospin projection $m$ and $\nu$. Thus, Eqs. (20a)–(20d) give the spin and isospin wave function of the nucleon ($N$), deuteron ($d$), triton and helion ($T$), and the $\alpha$ particle ($\alpha$).

### A. One-Particle Stripping and Pickup Reactions

The form factor $F$ appropriate to the one-nucleon pickup and stripping reactions can be given in terms of a single-particle bound-state wave function $\phi_{lj}$. We write this as[1]

$$F^{BC}_{lsj}(r) = \hat{s}^{-1} D_0(bc) \begin{cases} \phi_{lj}(r) & \text{(for stripping)} \\ \left(\frac{C}{B}\right)^3 \phi_{lj}\left(\frac{C}{B}r\right) & \text{(for pickup)}, \end{cases} \tag{23}$$

TABLE II. Values of the spectroscopic overlap integrals for inelastic and charge-exchange processes.

| Reaction | $\hat{\tau}^{-1}\hat{S}^{-1}\langle s_b \tau_b \| \mathcal{A}^\dagger_{S\mathcal{T}} \| s_a \tau_a\rangle$ |
|---|---|
| $(p,n)$ | 1 |
| $(d,d')$ | $\delta_{\tau 0}[\frac{1}{2}(s+3)(2-s)]^{1/2}$ |
| $(h,t)$ | $4\delta_{\tau 0}\delta_{s0} - (-)^{\tau+s}$ |
| $(\alpha,\alpha')$ | $2\delta_{s0}\delta_{\tau 0}$ |

where $D_0(bc)$ is the product of the overlap integral between the spin-isospin wave functions of the projectiles, and the zero-range constant $D_0$, i.e.,

$$D_0(bc) \equiv D_0 \left\langle s_c \middle\| \begin{Bmatrix} c^\dagger_{s\tau} \\ c_{\tilde{s}\tilde{\tau}} \end{Bmatrix} \middle\| s_b \right\rangle. \tag{24}$$

Using the spin-isospin wave function given in Eq. (20), we have calculated $D_0(bc)$ parameters and the results are summarized in Table I, together with the $D_0$ values assumed. The spectroscopic amplitude $\tilde{A}^{BC}_{lsj}$ can then be obtained from

$$\tilde{A}^{BC}_{lsj} \equiv \left\langle B \middle\| \begin{Bmatrix} c^\dagger_{lsj\tau} \\ c_{\tilde{l}\tilde{s}\tilde{j}\tilde{\tau}} \end{Bmatrix} \middle\| C \right\rangle, \tag{25}$$

where $c^\dagger_{lsjm\tau\nu}$ and $c_{lsjm\tau\nu}$ are the single-particle creation and annihilation operators of the single-particle state $(lsj\tau = \frac{1}{2})$ and

$$c_{\tilde{l}\tilde{s}\tilde{j}\tilde{m}\tilde{\tau}\tilde{\nu}} \equiv (-)^{j+m+\tau+\nu} c_{lsj-m\tau-\nu}. \tag{26}$$

### B. Inelastic and Charge-Exchange Reaction

We assume the effective two-body force given schematically by

$$\bar{V} = V(R,r)\{a_{11}(\vec{\sigma}\cdot\vec{\sigma})(\vec{\tau}\cdot\vec{\tau}) + a_{10}(\vec{\sigma}\cdot\vec{\sigma}) + a_{01}(\vec{\tau}\cdot\vec{\tau}) + a_{00}\} \tag{27}$$

for constructing the form factor for inelastic and charge-exchange reactions. Since the calculation

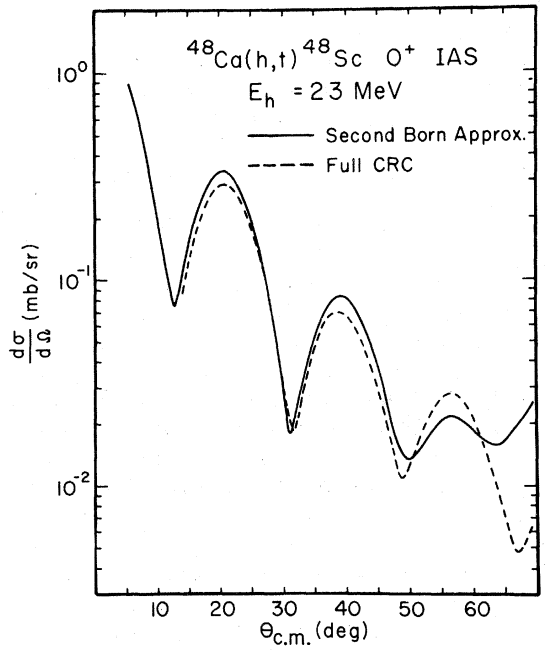


FIG. 1. A comparison of the results of a test calculation solving the coupled-reaction-channels (CRC) equations exactly (dashed line), with results of a calculation using the same parameters and the second Born approximation, as discussed in Sec. II (solid line).

of the form factor has already been shown in detail in Ref. 3, we only summarize here the necessary relations for numerical calculations. The produce of $\tilde{A}^{BC}_{lsj}$ and $F^{BC}_{lsj}(r)$ can be written as

$$\tilde{A}^{BC}_{lsj} F^{BC}_{lsj}(r) = 2\sqrt{2} \sum_{\tau \nu_1 \nu_2} a_{s\tau}(-)^{-\nu} \langle \tfrac{1}{2}\nu_1 \tfrac{1}{2}\nu_2 | \tau\nu\rangle (-)^{s_c - s_b} \hat{\tau}^{-1}\hat{s}^{-1} \langle s_b \tau_b \| \mathfrak{B}^{\dagger}_{s\tau} \| s_c \tau_c \rangle$$
$$\times (-)^{\tau_c - \nu_c} \langle \tau_c \nu_c \tau_b - \nu_b | \tau\nu\rangle \sum_{j_1 j_2} g^{12}_l(r) q^{12}_{lsj} \hat{j}^{-1} \langle J_B \| \mathfrak{B}^{\dagger}_j(j_1 j_2) \| J_C \rangle , \tag{28}$$

where

$$\mathfrak{B}^{\dagger}_{sm\tau\nu} \equiv \sum \langle \tfrac{1}{2} m_1 \tfrac{1}{2} m_2 | sm\rangle \langle \tfrac{1}{2}\nu_1 \tfrac{1}{2}\nu_2 | \tau\nu\rangle c^{\dagger}_{m_1\nu_1} c_{\tilde{m}_2 \tilde{\nu}_2} , \tag{29}$$

$$\mathfrak{B}^{\dagger}_{jm}(j_1 j_2) \equiv \sum \langle j_1 m_1 j_2 m_2 | jm\rangle c^{\dagger}_{j_1 m_1 \nu_1} c_{\tilde{j}_2 \tilde{m}_2 \tilde{\nu}_2} . \tag{30}$$

In Eq. (29) we only include the spin-isospin part of the wave function, while in Eq. (30) also the radial part is included. Finally, $g^{12}_l(R)$ and $q^{12}_{lsj}$ are the radial and spin-angle parts of the single-particle matrix element, defined, respectively, by

$$g^{12}_l(R) = \langle j_1 | \overline{V}_l(R, r) | j_2 \rangle ,$$
$$\overline{V}_l(R, r) = \int V(\vec{R}, \vec{r}) P_l(\cos\theta) d(\cos\theta) , \tag{31}$$

and

$$q^{12}_{lsj} = \langle j_1 \| (i^l Y_l \hat{\sigma}_s)_j \| j_2 \rangle . \tag{32}$$

The reduced matrix element $\langle s_b \tau_b \| \mathfrak{B}^{\dagger}_{s\tau} \| s_a \tau_a \rangle$ with respect to the projectiles were calculated, again using the wave functions given by Eq. (20). The results are contained in Table II.

## IV. RESULTS OF THE $(h, t)$ ANALYSES

The CRC formulation of Sec. II. embodied in the program JUPITER-4, has been used to study the two-step process via $\alpha$-particle channels [i.e., the pickup-stripping $(h, \alpha)$, $(\alpha, t)$ mechanism] as it contributes to the $^{40}$Ar$(h, t)^{40}$K and $^{48}$Ca$(h, t)^{48}$Sc reactions. Angular-distribution data are available at 35-MeV incident helion energy for the $0^+$ analog state (IAS) (4.38 MeV) and $0^+$ antianalog state (AAS) (1.65 MeV) in $^{40}$K,[6] and at 23-MeV incident helion energy for the $0^+$ analog state (6.67 MeV), and the $2^+$ (1.14-MeV), $4^+$ (0.25-MeV), and $6^+$ (ground) states in $^{48}$Sc.[20]

The $^{40}$Ar$(h, t)^{40}$K analysis is discussed in an earlier note[14] and relevant features will only be summarized here. A $^{48}$Ca$(h, t)^{48}$Sc analysis using the second Born approximation and assuming the mechanism is entirely $(h, \alpha)$, $(\alpha, t)$ has also been made previously by Toyama.[13]

We first want to comment upon the accuracy of the second Born approximation, which was used by Toyama[13] and also is used in the majority of the calculations described here. We have carried out a fully coupled reaction channel calculation for the $^{48}$Ca$(h, t)^{48}$Sc reaction to the $0^+$ analog state. The result is compared with that obtained by using the second Born approximation in Fig. 1. It is seen that the calculated cross section given by the second Born approximation is not much different from that given by the exact calculation. This implies that the second Born approximation is indeed a very good approximation for calculation of the two-step processes considered in the present work.

The most important aspect of the problem when two or more reaction mechanisms contribute is the interference between them. No investigation, excepting ours in Ref. 14, has so far been made of this effect. Thus the main interest of the present calculation is to study this interference.

### A. $^{40}$Ar$(h, t)^{40}$K

Turning to the specific case of $^{40}$Ar$(h, t)^{40}$K ($0^+$, IAS, 4.38 MeV and $0^+$, AAS, 1.65 MeV), we consider four intermediate states in $^{39}$Ar. These are the $f_{7/2}$ ground state and three $d_{3/2}$ two-particle–three-hole states. The first of these $d_{3/2}$ states is taken as the $d_{3/2}$ state at 1.52 MeV, the second is taken to have an excitation of 3.9 MeV, roughly the centroid of the higher $d_{3/2}$ hole strength in $^{39}$Ar,[22] and the third, with $T = \frac{5}{2}$, is assumed to lie at around 9.0 MeV in excitation, in the continuum. Spectroscopic amplitudes for the $(h, \alpha)$ transitions to, and $(\alpha, t)$ transitions from these states are given in Ref. 14. The uppermost $\frac{3}{2}^+$ state cannot contribute by stripping to the AAS, and the small stripping contribution of the 3.9-MeV $\frac{3}{2}^+$ state to the IAS was neglected. The separation-energy procedure was used to compute the form factors appropriate to these transitions, and also those considered in $^{48}$Ca$(h, t)^{48}$Sc.

Results of the calculations, for $^{40}$Ar$(h, t)^{40}$K using $h$ and $t$ optical parameters from the survey by Bechetti and Greenless[23] and the higher-energy $\alpha$ potential adopted by Toyama,[13] are presented in Fig. 2. The data are those of Hinrichs *et al.*,[6] at 35 MeV. In Fig. 2(a) are shown the conventional DWBA calculations (as dashed lines) and the pure pickup-stripping calculations, in second DWBA

(as solid lines). The microscopic form factor for the conventional DWBA calculations used a Gaussian two-body interaction with $\overline{V}=3$ MeV and $\beta=3.0$ fm, and included configuration mixing.[14] The $D_0$ value for $(h,\alpha)$ and $(\alpha,t)$ is based upon that suggested by Stock *et al.*,[24] namely $D_0=-4.8\times10^2$ MeV fm$^{3/2}$. It will be noted that the pickup-stripping calculation is the only one agreeing with the *shape* of the $0^+$ AAS angular distribution.

On the other hand, the relative *magnitudes* of conventional DWBA and second DWBA are quite different and the AAS/IAS ratios for the pickup-stripping cross sections are much too small. One would expect, *a priori*, that both the simple direct and the pickup-stripping mechanisms (among others) contribute to the observed angular distributions. Figure 2(b) shows the result of a summation of the amplitudes for both processes. In these calculations, $D_0$ was reduced to $-3.9\times10^2$ MeV fm$^{3/2}$ for $(h,\alpha)$ and $(\alpha,t)$, while $\overline{V}$, for the microscopic $(h,t)$ form factors, was reduced to 1.2 MeV. The resulting cross sections have magnitude agreeing well with the experimental cross sections.

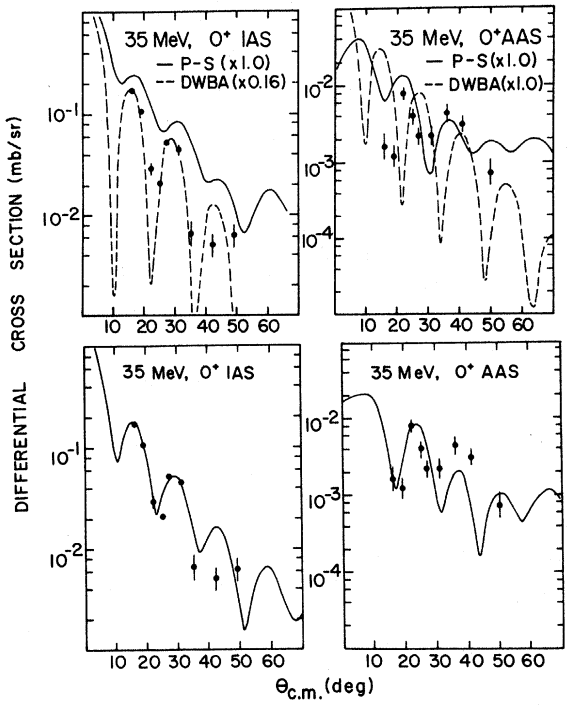


FIG. 2. The $^{40}$Ar$(h,t)^{40}$K ($0^+$, 4.38-MeV IAS and $0^+$, 1.65-MeV AAS) cross sections at 35 MeV. The experimental data are taken from Ref. 6. The calculated curves in the upper half of the figure are the results of direct (dashed line) and pickup-stripping (full line) calculations, as discussed in the text. The lower half of the figure shows the result (solid line) of taking both processes into account simultaneously. See also Ref. 14.

### B. $^{48}$Ca$(h,t)^{48}$Sc

For the two-step process in the $^{48}$Ca$(h,t)^{48}$Sc reaction we take into account only the ground state of $^{47}$Ca as the single intermediate state in the $\alpha$ channel. It is assumed that the final and the intermediate states are pure $(f_{7/2}^{-1}, f_{7/2})$ and $f_{7/2}^{-1}$ configurations, respectively. The target state is also assumed to be a closed-shell core. The spectroscopic amplitude, $\langle J_B \| \{c_j^\dagger\} \| J_A\rangle$, for the $(h,\alpha)$ and $(\alpha,t)$ processes are then easily calculated and the results are summarized in Table III. The form factor for the direct process was calculated by using the procedure summarized in Sec. III. The spectroscopic overlap integrals required, $\langle J_B \| \mathfrak{A}_j^\dagger \| J_A\rangle$, were evaluated from the wave functions of the pure $f_{7/2}$ particle-hole configurations and are given for $^{48}$Ca$(h,t)^{48}$Sc also in Table III.

The sets of optical-potential parameters used in the present $^{48}$Ca and $^{48}$Sc calculations are listed in Table IV. The parameters for $h$ and $t$ channels are taken from the work of Bechetti and Greenlees,[23] but the strengths of the imaginary parts of the potentials are reduced for $^{48}$Ca and $^{48}$Sc so that the calculated cross sections, including only the two-step processes, agree with the observed magnitude of the experimental $(h,t)$ cross sections. The parameters used for the $\alpha$-particle channels are taken from Stock *et al.*[24]

The calculated cross sections for the $0^+$, $2^+$, $4^+$, and $6^+$ states are shown in Figs. 3 and 4. For each case, three theoretical curves are drawn, which are obtained, respectively, by taking into account: (i) the two-step process only (full line), (ii) the direct process only (dot-dashed line), (iii) and both processes simultaneously (dotted line). The parameters used in calculation of the two-step process are given in Table IV and the strength of the two-body interaction for the direct reaction is taken as $\overline{V}=5.8$ MeV (with $\beta=2.3$ fm). These parameters are chosen so that either the two-step process or the direct reaction alone can explain the magnitude of the experimental $0^+$ cross section. Therefore, the direct-plus-two-step calculations also shown in Figs. 3 and 4 are not expected to fit the experimental data, but are in-

TABLE III. Values of the spectroscopic amplitudes for the direct and the pickup-stripping processes in $^{48}$Ca$(h,t)^{48}$Sc reaction.

| Process | Spectroscopic amplitude |
|---|---|
| $^{48}$Ca $0^+ \rightarrow {}^{47}$Ca $\frac{7}{2}^-$ | $\sqrt{8}$ |
| $^{47}$Ca $\frac{7}{2}^- \rightarrow {}^{48}$Sc $J^+$ | $-(2J+1)^{1/2}$ |
| $^{48}$Ca $0^+ \rightarrow {}^{48}$Sc $J^+$ | 1 |

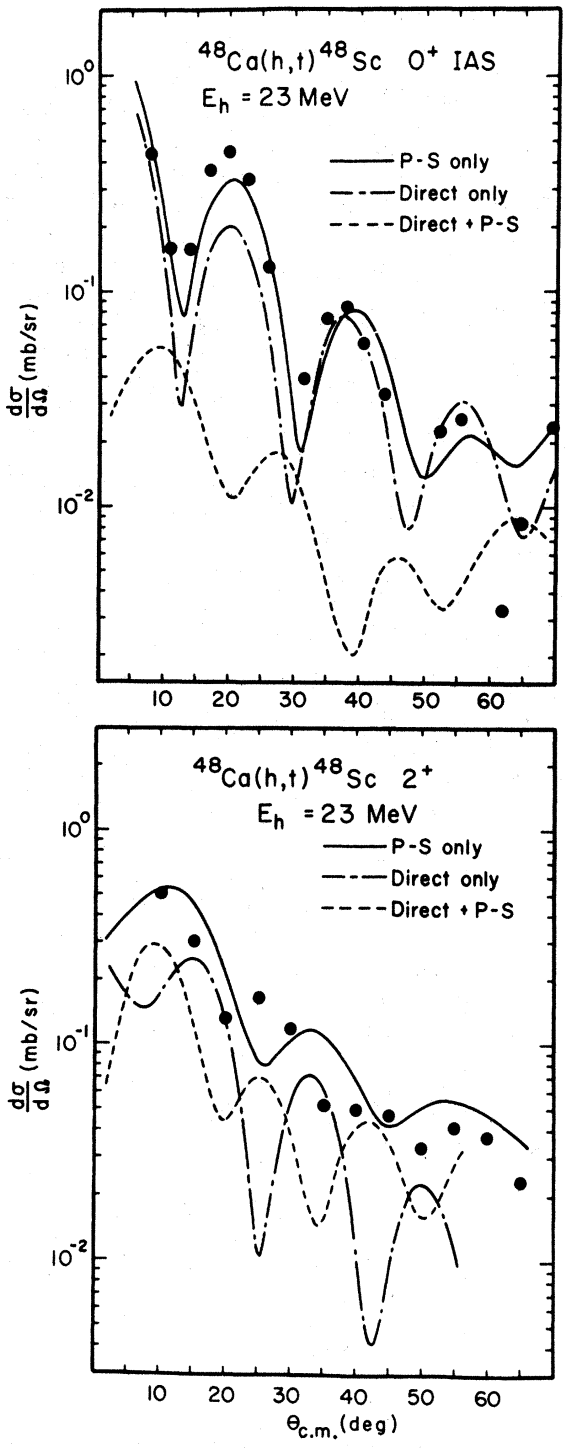


FIG. 3 Cross sections for $^{48}$Ca$(h,t)^{48}$Sc reactions at 23 MeV, populating the $0^+$ (6.67-MeV, IAS) and $2^+$ (1.14-MeV) levels. Experimental data are taken from Ref. 20. Theoretical predictions are shown for the direct process (dashed curve), the pure pickup-stripping process (dot-dashed curve), and for both processes simultaneously (full curve). The parameters are those given in Tables I–IV, with a direct interaction strength of $\overline{V}$=5.8 MeV.

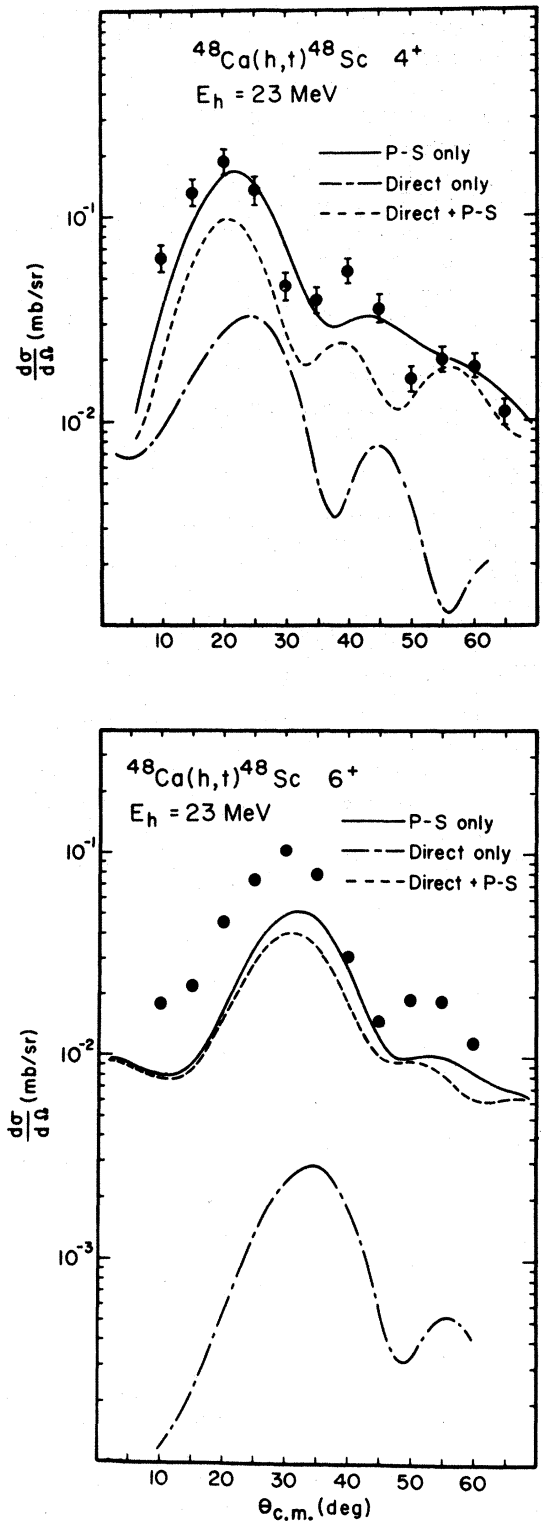


FIG. 4. The interpretation is as in Fig. 3, except that the experimental cross sections and calculations for the $4^+$ (0.25-MeV) and $6^+$ (ground) states are shown.

tended to illustrate the trends of the interference between the direct and two-step process for this case. As is seen, the interference is destructive for all four final states.

A pure $(h, \alpha)$, $(\alpha, t)$ process has previously been assumed in second Born-approximation calculations by Toyama[13] for the same reaction as we consider here. Our calculation confirms the result of Toyama, that the two-step process can explain both the relative magnitude and shape of the cross sections for $0^+$, $2^+$, $4^+$, $6^+$ states. However, the parameters used by Toyama are not strictly compatible with existing data at $E_h = 15$ MeV for the $^{48}$Ca$(h, \alpha)^{47}$Ca reaction.[25] In Fig. 5 we have plotted the absolute $^{48}$Ca$(h, \alpha)^{47}$Ca cross section for the ground state, calculated with the optical-model parameters used by Toyama,[13] in comparison with experiment. It is seen that the theoretical result is larger than the experimental data by about a factor of 1.7. Therefore if one readjusts, for instance, the $D_0$ parameter so that the $(h, \alpha)$ cross section is reproduced, the theoretical $(h, t)$ cross sections are reduced by a factor $1.7^2 = 2.9$, which destroys the agreement in magnitude obtained by Toyama.[26] One can also reproduce the $(h, \alpha)$ data by increasing the strength of the imaginary parts of the optical potentials. In this case, one obtains roughly the same amount of reduction of the $(h, t)$ reaction cross sections.

One might therefore consider that a better explanation of all the experimental data would be obtained if both the direct and indirect processes are taken into account simultaneously as in the $^{40}$Ar$(h, t)^{40}$K case. This is indeed possible, at least for the $0^+$ cross section. If one assumes a direct process about 2.5 times as strong as before, the experimental cross section can actually be reproduced as is indicated in Fig. 6. Assuming the stronger direct process is equivalent to assuming $\bar{V} = 14.5$ MeV for the effective force. To assume such a large $\bar{V}$, however, leads to a $2^+$ cross section about 1.5 times larger than experiment, as seen in Fig. 7. The shape of the $2^+$ curve is, however, considerably improved, illustrating the importance of the interference between direct and two-step processes.

The interference effects for the $4^+$ and $6^+$ states, on the other hand, are less important as a consequence of the fact that the direct transition amplitudes for these states are much smaller than those of the two-step processes as seen in Fig. 4. Even if the direct amplitude is doubled, the dominant process is still the two-step process. The effect of interference, however, is not completely negligible, particularly for the $4^+$ cross sections. When $\bar{V}$ is increased to 14.5 the cross section changes by a factor of 1.5, and therefore the direct process is important for the purpose

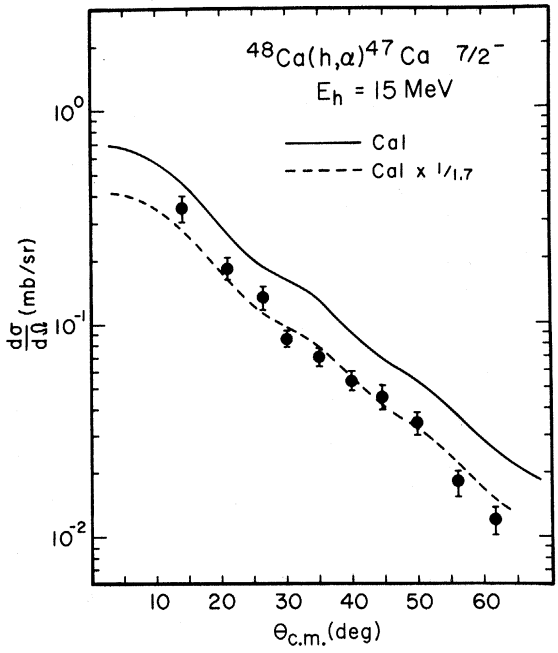


FIG. 5. Comparison of the experimental cross section for $^{48}$Ca$(h, \alpha)^{47}$Ca (ground state), at 15 MeV, with the predictions of DWBA using the optical parameters of Toyama, Ref. 13. Data are from Ref. 25.

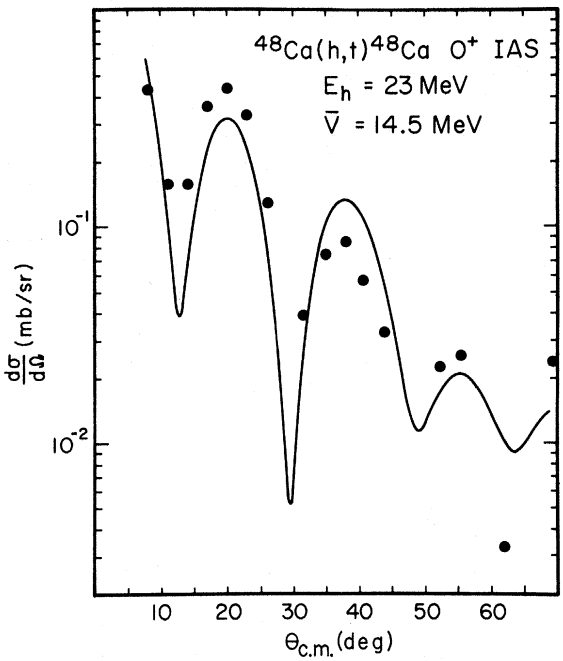


FIG. 6. Cross sections for the $^{48}$Ca$(h, t)^{48}$Sc reaction populating the $0^+$ (6.67-MeV, IAS) state, the data being from Ref. 20 and the calculation a direct plus pickup-stripping CRC calculation, with the direct interaction strength $\bar{V} = 14.5$ MeV.

of quantitative discussions.

It should be remarked, also, that in the present $^{48}Ca(h, t)^{48}Sc$ calculations we as well as Toyama[13] neglected configuration mixing in the nuclear states involved in the reaction. In this respect it is interesting to consider the effect of configuration mixing in the $^{40}Ar(h, t)^{40}K$ calculations, due to the fact that the analog and antianalog states are a linear combination of two components. This in turn leads to the necessity to consider three intermediate states. In Fig. 8 we show, for example, the two-step cross section for the $0^+$ AAS if the $^{39}Ar$ ground state only is included as the intermediate state. It is seen that the calculated cross section is completely changed both in shape and magnitude. We thus conclude that the interference of intermediate paths is very important in the two-step processes.

An analogous effect can be expected in the $^{48}Ca(h, t)^{48}Sc$ reaction. Consider, for example, the $2^+$ state. It is well known that in many nuclei configuration mixing of particle-hole states with $T=0$ leads to low-lying $2^+$ states, which carry most of the transition strength, and which are strongly excited in inelastic scattering. Similarly in the $(h, t)$ reaction the final states are particle-hole states with $T=1$, but because the $T=1$ force is repulsive, the collective $2^+$, $T=1$ state is expected to have higher energy. Therefore, the transition strength to low-lying $2^+$, $T=1$ states should be strongly reduced, as actually observed for the $T=1$ dipole transitions.[27] This reduction is brought about by destructive interference due to configuration mixing. A possibility thus exists that we can further improve the fit to the $^{48}Ca(h, t)^{48}Sc$, $2^+$ cross sections by considering configuration mixing effects, and such a calculation is in progress.

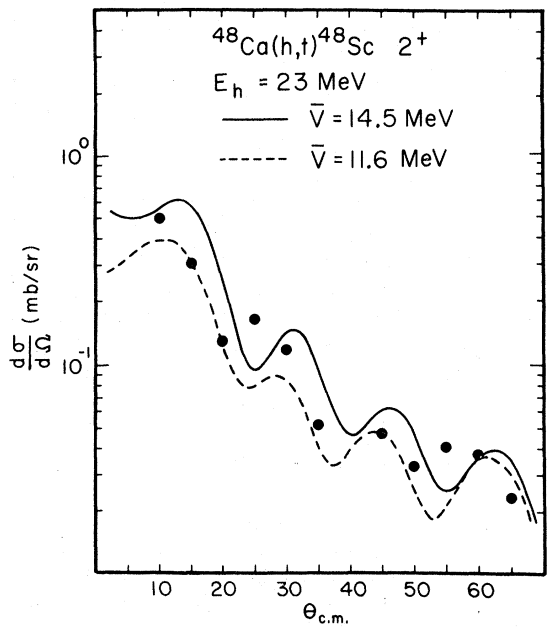


FIG. 7. As in Fig. 6, but for the cross section to the $2^+$ (1.14-MeV) state in $^{48}Sc$.

## V. CONCLUDING REMARKS

Using the CRC formalism of Sec. II and the form-factor conventions of Sec. III we presented in Sec. IV a study of the two-step $(h, \alpha)$, $(\alpha, t)$ contribution to $(h, t)$, and particularly the interference of this reaction mode with the familiar direct $(h, t)$ process. In both reactions studied, $^{40}Ar(h, t)^{40}K$ and $^{48}Ca(h, t)^{48}Sc$, the interference is destructive, except if the final state is the $0^+$ AAS.

Two ingredients are crucial in determining the nature of the interference: the distorted wave functions for the intermediate $\alpha$-particle channels; and, the relative phase of the dynamic spectroscopic amplitude of the direct process, $\langle J_B \| \mathfrak{B}_j^\dagger \| J_A \rangle$, with respect to that of the product of the amplitudes for the pickup-stripping process, $\langle J_B \| c_{j_2}^\dagger \| J_C \rangle \langle J_c \| c_{j_1} \| J_A \rangle$.

The first of these ingredients arise in a very

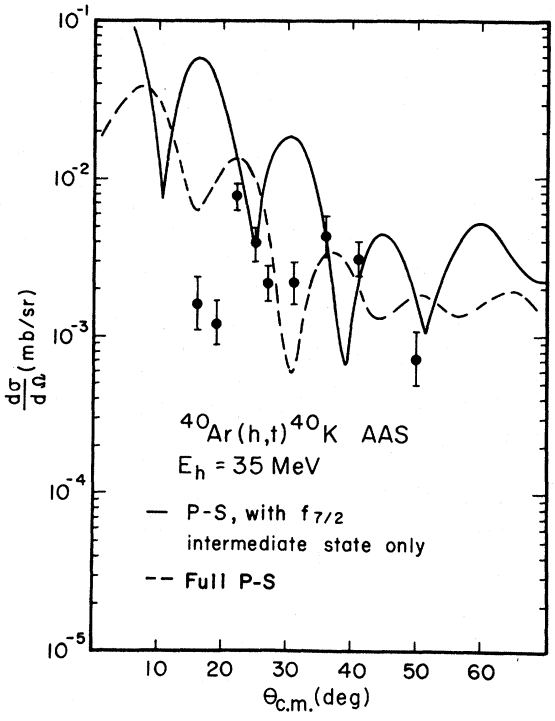


FIG. 8. Cross section for the $^{40}Ar(h, t)^{40}K$ reaction to the $0^+$ (1.65-MeV, AAS) state, as in Fig. 2. The dashed curve is the pickup-stripping calculation, also shown in Fig. 2, with three intermediate $^{39}Ar$ states. The full curve is a similar calculation in which the only intermediate state included is the ground state of $^{39}Ar$.

TABLE IV. Optical and binding potential parameters used in the present analysis of $^{48}$Ca$(h,t)^{48}$Sc. The strengths of the binding potentials were adjusted to reproduce the experimental separation energies.

| Projectile | $V$ | $W$ | $a$ | $a_I$ | $r$ | $r_I$ | $r_c$ |
|---|---|---|---|---|---|---|---|
| $h$ | 156.2 | 26.8 | 0.72 | 0.88 | 1.2 | 1.4 | 1.3 |
| $t$ | 161.5 | 21.8 | 0.72 | 0.84 | 1.2 | 1.4 | 1.3 |
| $\alpha$ | 183.7 | 26.0 | 0.56 | 0.56 | 1.4 | 1.48 | 1.4 |
| $n$ | | | 0.65 | | 1.25 | | |
| $p$ | | | 0.65 | | 1.25 | | 1.25 |

complicated way. But the distorted waves are relatively insensitive to target mass and channel energy, so that the character of the interference is a slow function of mass and energy. Thus we feel that the similarity to, or difference of, our present results and similar analyses applied to other nuclei can generally be understood by a study of the spectroscopic amplitudes involved.

Without specifying the amplitudes explicitly it is possible to ascertain the nature of the interference with the help of a sum rule,

$$\hat{J}_B^{-1}\langle J_B\|\mathfrak{B}_j^\dagger(j_p,j_n)\|J_A=0\rangle = \delta_{jJ_B}(-)^{j_p+j_n-j}\sum_{J_C}\delta_{j_pJ_C}\hat{J}_C^{-1}\hat{J}_B^{-1} \times\langle J_B\|c_{j_p}^\dagger\|J_C\rangle\langle J_C\|c_{\tilde{j}_n}\|J_A=0\rangle, \tag{33}$$

where the left-hand side is the spectroscopic amplitude for the direct charge-exchange process, $j_n\to j_p$, multiplied by a factor $\hat{J}_B^{-1}$. The right-hand side of the equation is essentially the sum of the products of the spectroscopic amplitudes of the successive pickup (of a neutron in a $j_n$ orbit) and stripping (of a proton to the $j_p$ orbit) processes. Note that the relation (33) was derived assuming explicitly that the spin of the target nucleus is zero ($J_A=0$).

The usefulness of the relation (33) may be seen by applying it to the $(h,t)$ reaction populating the IAS. Since $J_B=0$ for this case, the relation reduces to

$$\langle\mathrm{IAS}\|\mathfrak{B}_0^\dagger(j_p,j_n)\|0\rangle = -j_p^{-1}\delta_{j_pj_n}\sum_{J_C}\langle\mathrm{IAS}\|c_{j_p}^\dagger\|J_C=j_n\rangle\langle J_C\|c_{\tilde{j}_n}\|0\rangle. \tag{34}$$

Very often, we have the situation where only one intermediate state is allowed for the two-step process [as in the case of $^{48}$Ca$(h,t)^{48}$Sc considered here]. Then, the relation is further simplified, to

$$\langle\mathrm{IAS}\|\mathfrak{B}_0^\dagger(j_p,j_n)\|0\rangle = -\hat{j}_p^{-1}\delta_{j_pj_n}\langle\mathrm{IAS}\|c_{j_p}^\dagger\|j_n\rangle\langle j_n\|c_{\tilde{j}_n}\|0\rangle. \tag{35}$$

If we define

$$R=\langle J_B\|\mathfrak{B}_j^\dagger\|J_A\rangle/[\langle J_B\|c_{j_2}^\dagger\|J_C\rangle\langle J_C\|c_{j_1}\|J_A\rangle], \tag{36}$$

it is seen from Eq. (35) that $R$ is negative, irrespective of the orbit $j_n$ ($=j_p$) and the nucleus involved. Thus we will observe a very similar interference between the direct and the two-step processes, for all the possible $j_n\to j_p$, transitions contributing to the excitation of the IAS in any nucleus. This conclusion does not change, even if more than one intermediate state is contributing, since the relation holds for the net contribution. Summarizing the preceding arguments, one may conclude that for the IAS, we will observe destructive interference over a wide range of nuclei and intermediate $\alpha$-particle energies. In a similar way, one may use the sum rule (33) to discuss the character of the interference in other cases.

In interpreting some of the experimental data, as for instance the $^{40}$Ar$(h,t)^{40}$K reaction leading to the AAS and the $^{48}$Ca$(h,t)^{48}$Sc, $2^+$ cross section, it is important to include realistically the configuration mixing in the nuclear states involved in the reaction. It is generally much easier to predict the effects of configuration mixing for the direct process, than for the two-step process. In this connection, it is interesting to note that the sum rule also gives us some information on this point. For instance, consider the excitation of the $2^+$ state in the $^{48}$Ca$(h,t)^{48}$Sc reaction, and suppose that the $f_{7/2}^{-1}p_{3/2}$ state is mixed into the final $2^+$ state consisting mainly of the $f_{7/2}^{-1}f_{7/2}$ configuration. The $2^+$ state can then be excited either though the $f_{7/2}\to f_{7/2}$ transition or though the $f_{7/2}\to p_{3/2}$ transition. From Eq. (33), it is easy to see that the values of $R$ for both cases are the same. This implies that the nature of the interference between the direct and the two-step process is the same in both cases: If one observes destructive interference between them for the $f_{7/2}\to f_{7/2}$ transition, one also observes destructive interference for the $f_{7/2}\to p_{3/2}$ transition.

It would be desirable to conclude with some very general statements concerning the importance of two-step-transfer processes in charge-exchange reactions. However, we do not feel that this is presently possible, and instead we want to stress the theoretical ambiguities inherent in the present, and earlier, calculations for both the

direct and two-step process. The effective force which is responsible for the direct process is obviously not well known, because it is usually obtained from experiment without taking two-step processes into consideration, and clearly these may not be neglected in general. On the other hand, the way to calculate the two-step process is far from established. The neglect of non-orthogonality corrections between channels with different mass partitions, as well as the use of the zero-range approximation, could well introduce considerable error. Also, the zero-range parameters $D_0$ for the $(h, \alpha)$ and $(\alpha, t)$ reactions are not well known, nor does one know the systematic behavior of optical potentials in the $h$ and $t$ channels. At the present stage we are not yet able to separate clearly the influence of these various possible sources of ambiguity, especially because in many cases the angular distributions for the direct and two-step processes have the same shape (see e.g., Fig. 3). A search of available data for reactions presenting a more crucial test of the two-step mechanism, or new experiments constituting such a test, will be needed to clarify many of the thorny issues we have encountered in the present work.

*Note added in proof:* A study of interference between direct and multistep processes has also been made recently by Toyama and co-workers. We are indebted to Dr. Toyama for his kind communication of prepublication results.

---

*Work supported in part by the U. S. Atomic Energy Commission.

†Work supported by Heinrich-Hertz-Stiftung, Nordrhein-Westfalen, Germany.

[1]G. R. Satchler, Nucl. Phys. 55, 1 (1964).

[2]G. R. Satchler, R. M. Drisko, and R. H. Bassel, Phys. Rev. 136, B637 (1964).

[3]V. A. Madsen, Nucl. Phys. 80, 177 (1966).

[4]E. Rost and P. D. Kunz, Phys. Letters 30B, 231 (1969).

[5]P. Kossanyi-Demay, P. Roussel, H. Farraggi, and R. Schaeffer, Nucl. Phys. A148, 181 (1970).

[6]R. A. Hinrichs, R. Scherr, G. M. Crawley, and I. Proctor, Phys. Rev. Letters 25, 829 (1970).

[7]J. R. Comfort, J. P. Schiffer, A. Richter, and M. M. Stautberg, Phys. Rev. Letters 26, 1338 (1971).

[8]R. A. Hinrichs and G. F. Trentelman, Phys. Rev. C 4, 2079 (1971).

[9]R. Schaeffer, Argonne Physics Division Informal Report No. RHY-1970A (unpublished).

[10]W. L. Fadner, J. J. Kraushaar, and L. C. Farwell, Nucl. Phys. A178, 385 (1972); see also G. W. Hoffmann *et al.*, Phys. Letters 40B, 453 (1972).

[11]W. L. Fadner, J. J. Kraushaar, and S. I. Hayakawa, Phys. Letters 40B, 49 (1972).

[12]R. Schaeffer and G. Bertsch, Phys. Letters 38B, 159 (1972).

[13]M. Toyama, Phys. Letters 38B, 147 (1972).

[14]W. R Coker, T. Udagawa, and H. H. Wolter, Phys. Letters 41B, 237 (1972).

[15]N. K. Glendenning, in *Proceedings of the International Conference on Properties of Nuclear States,* edited by M. Harvey (Presses de l'Université de Montréal, Montréal, Canada, 1969); R. J Ascuitto and N. K. Glendenning, Phys. Rev. C 4, 1260 (1970); T. Tamura, D. R. Bes, R. A. Broglia, and S. Landowne, Phys. Rev. Letters 25, 1507 (1970); 26, 156(E) (1971); R. J. Ascuitto, N. K. Glendenning, and B. Sorensen, Phys. Letters 34B, 17 (1971); Nucl. Phys. A183, 60 (1972); T. Udagawa, T. Tamura, and T. Izumoto, Phys. Letters 35B, 129 (1971).

[16]T. Omura, B. Imanishi, M. Ichimura, and M. Kawai, Progr. Theoret. Phys. (Kyoto) 44, 1242 (1970).

[17]L. J. B. Goldfarb and K. Takeuchi, Nucl. Phys. A181, 609 (1972).

[18]A. Stamp, Nucl. Phys. 83, 232 (1969); R. J. Ascuitto, N. K. Glendenning, and B. Sorensen, *ibid.* A170, 65 (1971).

[19]T. Tamura, Rev. Mod. Phys. 37, 679 (1965).

[20]A. Richter, J. R. Comfort, N. Anantaraman, and J. P. Schiffer, Phys. Rev. C 5, 821 (1972).

[21]T. Tamura, Oak Ridge National Laboratory Report No. ORNL-4152, 1967 (unpublished); H. Wolter (unpublished).

[22]W. Fitz, R. Jahr, and R. Santo, Nucl. Phys. A114, 392 (1968).

[23]F. D. Bechetti and G. W. Greenlees, in *Polarization Phenomena in Nuclear Reaction,* edited by H. H. Barschall and W. Haeberli (University of Wisconsin Press, Madison, 1971), p. 682.

[24]R. Stock, R. Bock, P. David, H. Duhm, and T. Tamura, Nucl. Phys. A104, 136 (1967).

[25]C. M. Fou and R. W. Zurmuhle, Nucl. Phys. A129, 138 (1969).

[26]Our calculated two-step $(h,t)$ cross sections turn out to be systematically smaller than those reported by Toyama, by about a factor of 0.625, for all residual states, when the published parameters of Toyama are used. We do not know the origin of this discrepancy between the two independent calculations; however, it does not affect our general conclusions.

[27]D. F. Peterson and C. J. Veje, Phys. Letters 24B, 449 (1967).